

REFERENCES

1. Abou-Alfa GK, Jarnagin W, Lowery M, et al. Liver and bile duct cancer. In: Niederhuber JE, Armitage JO, Doroshow JH, et al., editors. *Abeloff's clinical oncology*. 5th ed. Philadelphia: Elsevier Saunders; 2014. p. 1373–96.
2. Szejnfeld D, Nunes TF, Fornazari VAV, et al. Transcatheter arterial embolization for unresectable symptomatic giant hepatic hemangiomas: single-center experience using a lipiodol-ethanol mixture. *Radiol Bras*. 2015;48:154–7.
3. Bormann RL, Rocha EL, Kierzenbaum ML, et al. The role of gadoteric acid as a paramagnetic contrast medium in the characterization and detection of focal liver lesions: a review. *Radiol Bras*. 2015;48:43–51.
4. Candido PCM, Pereira IMF, Matos BA, et al. Giant pedunculated hemangioma of the liver. *Radiol Bras*. 2016;49:57–8.
5. Giardino A, Miller FH, Kalb B, et al. Hepatic epithelioid hemangioendothelioma: a report from three university centers. *Radiol Bras*. 2016; 49:288–94.
6. Gaddikeri S, McNeely MF, Wang CL, et al. Hepatocellular carcinoma in the noncirrhotic liver. *AJR Am J Roentgenol*. 2014;203:W34–47.
7. Hennedige T, Venkatesh SK. Imaging of hepatocellular carcinoma: diagnosis, staging and treatment monitoring. *Cancer Imaging*. 2013; 12:530–47.
8. Chung YE, Park MS, Park YN, et al. Hepatocellular carcinoma variants: radiologic-pathologic correlation. *AJR Am J Roentgenol*. 2009; 193:W7–13.
9. Ros PR, Erturk SM. Malignant tumors of the liver. In: Gore RM, Levine MS, editors. *Textbook of gastrointestinal radiology*. 4th ed. Philadelphia: Elsevier Saunders; 2015. p. 1561–607.
10. Kimura H, Inoue T, Konishi K, et al. Hepatocellular carcinoma presenting as extrahepatic mass on computed tomography. *J Gastroenterol*. 1997;32:260–3.
11. Horie Y, Katoh S, Yoshida H, et al. Pedunculated hepatocellular carcinoma. Report of three cases and review of literature. *Cancer*. 1983;51: 746–51.
12. Roumanis PS, Bhargava P, Kimia-Aubin G, et al. Atypical magnetic resonance imaging findings in hepatocellular carcinoma. *Curr Probl Diagn Radiol*. 2015;44:237–45.
13. Longmaid HE 3rd, Seltzer SE, Costello P, et al. Hepatocellular carcinoma presenting as primary extrahepatic mass on CT. *AJR Am J Roentgenol*. 1986;146:1005–9.
14. Winston CB, Schwartz LH, Fong Y, et al. Hepatocellular carcinoma: MR imaging findings in cirrhotic livers and noncirrhotic livers. *Radiology*. 1999;210:75–9.

**Glaucio Rodrigo Silva de Siqueira<sup>1</sup>, Marcos Duarte Guimarães<sup>2</sup>, Luiz Felipe Sias Franco<sup>1</sup>, Rafaela Batista e Silva Coutinho<sup>1</sup>, Edson Marchiori<sup>3</sup>**

1. Hospital Heliópolis, São Paulo, SP, Brazil. 2. A.C. Camargo Cancer Center, São Paulo, SP, Brazil. 3. Universidade Federal do Rio de Janeiro (UFRJ), Rio de Janeiro, RJ, Brazil. Mailing address: Dr. Glaucio Rodrigo Silva de Siqueira. Rua Inácio Manuel Álvares, 1000, Bloco 2, ap. 24, Jardim Ester. São Paulo, SP, Brazil, 05372-111. E-mail: glauciosiqueira@yahoo.com.br

<http://dx.doi.org/10.1590/0100-3984.2015.0118>

**Spondylometaphyseal dysplasia: an uncommon disease**

Dear Editor,

A 2-year-old female patient, born by normal delivery, without complications, at 39 weeks of gestation, all prenatal test results having been normal, was referred to the department of orthopedics and traumatology for investigation of deformities of the thorax and ankle, as well as dwarfism. She showed no psychomotor alterations. The parents of the child were healthy, with no history of malformations, and the patient was their only child. They reported that the child had been born with dental precocity, with 9 teeth at birth, and began to present changes in the thorax and ankles at 4 months of age, those changes progressing thereafter. They also reported that the child had not grown, having been 75 cm tall since the age of 1 year and the same weight, approximately 9 kg, since the age 9 months, both of those measurements, according to the US CDC, being below the 5th percentile.

Physical examination of the patient showed a prominent sternum and shortening of the trunk, as well as discrete coxa vara with rotation to the right, flat feet, and deformity of the wrists (Figures 1A and 1B). On X-rays, we observed metaphyseal deformities such as bone rarefaction, aerated bone containing trabeculae, and cortical irregularity, as well as right-sided scoliosis and deformities of the ribs (Figures 1C and 1D). Using Todd's Atlas of Skeletal Maturation as a reference, we determined the bone age to be 21 months. Computed tomography scans (not shown) of the cervical spine and of the head, respectively, showed discrete hypoplasia of the odontoid process and a reduction in the amount white matter around the posterior horn of the lateral ventricles, neither of which have been reported in the literature.

Spondylometaphyseal dysplasia (SMD) was first described in 1967 by Kozlowski et al.<sup>(1)</sup>, who defined it as a rare new form of bone dysplasia comprising various types of chondrodystrophy characterized by metaphyseal irregularities of the long bones, together with generalized platyspondyly of varying severity in the spine<sup>(1,2)</sup>. It produces a phenotypic spectrum of disorders, genotypically being autosomal dominant<sup>(3)</sup>. Kozlowski-type SMD, also known as type 1 SMD, is the most common form of the disease<sup>(1)</sup>.



**Figure 1.** A,B: Physical examination showing a prominent sternum (A) and flat feet (B). C,D: X-rays showing platyspondyly and deformities of the ribs (C), as well as metaphyseal deformations such as bone rarefaction, aerated bone containing trabeculae, and cortical irregularity (D).

The symptoms of SMD vary depending on the age of the patients<sup>(1)</sup>, the principal symptoms being as follows: limited postnatal growth; rhizomelic shortening of the limbs in early childhood evolving to shortening of the trunk by the age of 10 years; thoracic hypoplasia, which causes respiratory problems in the neonatal period and increases susceptibility to respiratory tract infection<sup>(4)</sup>; scoliosis with dorsal kyphosis; abnormalities of the metaphyses and pelvis<sup>(5)</sup>; odontoid hypoplasia; and valgus of the knees and claudication<sup>(6)</sup>, the latter typically being the first sign of the disease<sup>(2)</sup>. There might be little or no ossification of the cervical vertebrae, leading to cervical instability and swan neck deformity<sup>(7)</sup>.

A review of the literature revealed that there are currently 10 recognized subtypes of SMD. However, there is no consensus in the medical literature regarding those subtypes, because they are based on characteristics that are minimally different. Some subtypes are based on reports of only one case, and others can be diagnosed only after years of follow-up, which is difficult. For example, the longest follow-up period in a report of Sedaghatian-type SMD was 161 days. Therefore, there is no acceptable standard for subclassifying the disease.

REFERENCES

1. Nural MS, Diren HB, Sakarya O, et al. Kozlowski type spondylometaphyseal

dysplasia: a case report with literature review. *Diagn Interv Radiol.* 2006;12:70–3.  
 2. Jones KL. *Smith's Recognizable patterns of human malformation.* 6th ed. Philadelphia: Elsevier Saunders; 2006.  
 3. Nemeč SF, Cohn DH, Krakow D, et al. The importance of conventional radiography in the mutational analysis of skeletal dysplasias (the TRPV4 mutational family). *Pediatr Radiol.* 2012;42:15–23.  
 4. Suzuki S, Kim OH, Makita Y, et al. Axial spondylometaphyseal dysplasia: additional reports. *Am J Med Genet A.* 2011;155A:2521–8.  
 5. Krakow D, Vriens J, Camacho N, et al. Mutations in the gene encoding the calcium-permeable ion channel TRPV4 produce spondylometaphyseal dysplasia, Kozlowski type and metatropic dysplasia. *Am J Hum Genet.* 2009;84:307–15.  
 6. Ferrari D, Sudanese A. Spondylometaphyseal dysplasia: description of a case. *Chir Organi Mov.* 1994;79:325–9.  
 7. Simon M, Campos-Xavier AB, Mittaz-Crettol L, et al. Severe neurologic manifestations from cervical spine instability in spondylomegaphyseal-metaphyseal dysplasia. *Am J Med Genet C Semin Med Genet.* 2012;160C: 230–7.

Márcio Luís Duarte<sup>1</sup>, Élcio Roberto Duarte<sup>2</sup>, Daniela Brasil Solorzano<sup>2</sup>, Edgar Brasil Solorzano<sup>2</sup>, Jael Brasil de Alcântara Ferreira<sup>2</sup>

1. WebImagem, São Paulo, SP, Brazil. 2. Brasil Imagem Medicina Diagnóstica, Santos, SP, Brazil. Mailing Address: Dr. Márcio Luís Duarte. Avenida Ana Costa, 259, Gonzaga. Santos, SP, Brazil, 11060-001. E-mail: marcioluisduarte@gmail.com.

<http://dx.doi.org/10.1590/0100-3984.2015.0159>

Multiple primary malignancies: synchronous urothelial carcinoma of the bladder and adenocarcinoma of the colon

Dear Editor,

A 75-year-old White male presented with a three-month history of pain in the left hypochondrium. The patient also reported experiencing an episode of gross hematuria six months prior. He had quit smoking 20 years prior, having previously smoked 30 cigarettes/day for 30 years. He had also undergone surgery for a gastric ulcer 20 years prior. He reported no other comorbidities.

Computed tomography of the abdomen showed a solid, irregular, concentric mass, which was expansive and stenotic, in the middle third of the descending colon (Figures 1A and 1B). The mass showed heterogeneous uptake of the intravenous iodinated contrast medium and increased density of adjacent fat tissue, suggesting that it had expanded through the serosa. In addition, a vegetative lesion, with irregular borders and showing contrast enhancement, was observed in the right posterolateral wall of the bladder (Figures 1B and 1C).

Colonoscopy with biopsy of the intestinal mass led to a histological diagnosis of moderately differentiated adenocarcinoma of the colon, and the patient was therefore submitted to segmental colectomy with colostomy. The anatomopathological study revealed a hard, annular tumor, which was ulcerative and vegetative, infiltrating the intestinal wall and surrounding fat, thus confirming the result of the microscopy study of the biopsy. Subsequently, ultrasound of the urinary tract confirmed bladder nodulation (Figure 1D), with no perceptible flow on color Doppler. Complete transurethral resection of the nodulation was performed, and histopathological analysis of the resected specimen led to a diagnosis of superficial low-grade papillary urothelial carcinoma (World Health Organization grade I). A subsequent computed tomography scan of the abdomen and pelvis, for staging, showed no suspicious lesions. The final diagnosis was multiple, synchronous primary malignancies, probably secondary to smoking.

Colon cancer is the fourth most common malignancy in men, accounting for 90% of the cases that occur after the fifth decade of life, adenocarcinoma being the most common type<sup>(1)</sup>.

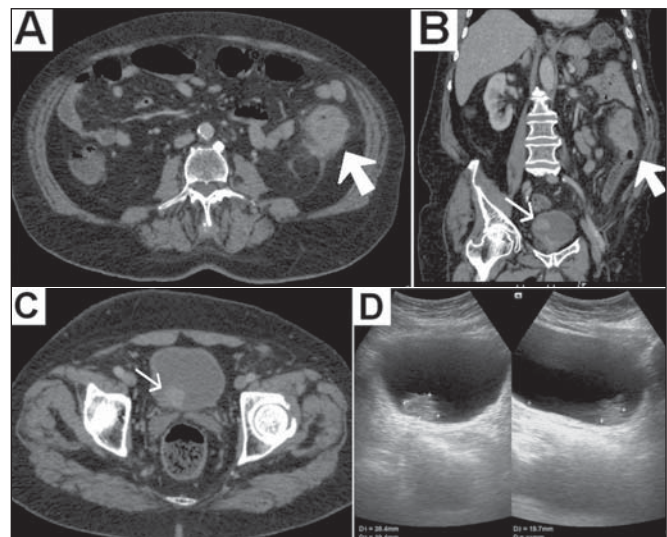


**Figure 1.** A,B: Computed tomography scan of the abdomen, obtained in the portal phase after intravenous administration of contrast medium, in an axial view (A) and oblique coronal reconstruction (B), showing a solid, irregular, concentric mass, which was expansive and stenotic, in the descending colon, presenting heterogeneous enhancement, together with increased density of the adjacent fat tissue (large arrow). Note also the vegetative lesion, with irregular borders and showing contrast enhancement (small arrow in B). C: Axial computed tomography slice, obtained in the portal phase after intravenous administration of iodinated contrast medium, showing the vegetative lesion, with irregular borders, located in the right posterolateral wall of the bladder (arrow). D: Abdominal ultrasound, confirming the lesion in the bladder wall.

In 5–10% of cases, adenocarcinoma is associated with hereditary syndromes (e.g., familial adenomatous polyposis, hereditary non-polypoid colorectal cancer, etc.), especially in young adults<sup>(1)</sup>. It is related to obesity, a sedentary lifestyle, a diet low in fiber, and inflammatory bowel diseases<sup>(1–4)</sup>. Smoking and alcoholism can also play roles<sup>(2–4)</sup>.

Bladder cancer, which is the most common type of malignant neoplasia of the urinary tract, affects individuals 55–60 years